Mechanical model to simulate the NSM FRP strips shear strength contribution to a RC beam: influence of each parameter on the force transferred by a single strip to a prism of plain concrete

V. Bianco & G. Monti
Dept. of Structural Engrg. and Geotechnics, Sapienza University, via A. Gramsci 53, 00197 Rome, Italy.

Joaquim A. O. Barros
Dept. of Civil Engineering, University of Minho, Campus de Azurém, 4800-058 Guimarães, Portugal.

ABSTRACT: A mechanical model, recently developed to simulate the shear strength contribution provided by a system of Near Surface Mounted (NSM) Fiber Reinforced Polymer (FRP) strips to a Reinforced Concrete (RC) beam throughout its loading process, is applied focusing on the behavior of a single NSM FRP strip orthogonal to the Critical Diagonal Crack (CDC). Firstly, attention is focused on the bond-based behavior of the strip mounted on the relevant prism of surrounding concrete. The influence of each parameter on the peak force transferable through bond stresses to the surrounding concrete, excluding the possibility of either concrete fracture and strip rupture, is analyzed. In the second part of the paper attention is focused on the comprehensive behavior of the strip: the influence of each parameter on the peak force transferable to the surrounding concrete, also including the possibility of both concrete fracture and strip rupture, is analyzed.

1 INTRODUCTION

Shear strengthening of RC beams by NSM technique consists in gluing FRP strips by an adhesive into thin shallow slits cut onto the concrete cover of the beam web lateral faces. A three dimensional mechanical model was recently developed to simulate the NSM FRP strips shear strength contribution to a RC beam (Bianco 2008, Bianco *et al.* 2009a-b). That model was developed fulfilling equilibrium, kinematic compatibility and constitutive laws of both materials – FRP and concrete – and bond between themselves. That model assumes that, during the loading process of a RC beam strengthened in shear by the NSM technique, the strips effectively crossing the CDC oppose its widening by anchoring to the surrounding concrete to which they transfer, through bond stresses, the force originating at their intersection with the CDC. The relative movement of the two parts into which the CDC divides the beam web, imposes on the strips' available resisting bond lengths an increasing end slip. As function of the relative mechanical and geometrical properties characterizing the specific case at hand, the ultimate configuration assumed by each strip can be: a) complete extraction of the NSM FRP strip due to loss of bond throughout the strip available resisting bond length, in case concrete mechanical properties are very high, which is indeed a very limit situation (debonding), b) concrete semi-conical fracture that reaches the strip free extremity (concrete semi-conical failure), c) concrete semi-conical fracture that stops progressing midway between loaded and free end, with consequent debonding of the remaining portion of the available bond length (mixed-semi-cone-plus-debonding) and d) rupture of the strip independently of an initial concrete fracture (strip rupture). In the first part of the paper, the model is applied to evaluate the influence of each geometrical/mechanical parameter on the peak force that a strip, near surface mounted on a concrete prism and subjected to an increasing imposed end slip, can transfer, through bond stresses, to the surrounding concrete. To that aim, the deformability of the concrete prism is accounted for while the possibilities of either concrete fracture or strip rupture are excluded by assuming the tensile strength of both materials, concrete and FRP, infinitely large. In the second part of the paper, the model is applied to evaluate the influence of each parameter on the peak load that a single strip can comprehensively transfer to the surrounding concrete, accounting also for the possibilities of occurrence of either concrete semi-conical tensile fracture or strip tensile rupture.

2 BOND-BASED BEHAVIOR OF A SINGLE NSM FRP STRIP

2.1 *Bond-based constitutive law*

Applying the model to the case of a single NSM FRP strip mounted on the surface of a concrete prism (Fig. 1), and neglecting the possibilities of both concrete semi-conical tensile fracture and strip

rupture, it is possible to determine the bond-based constitutive law of the strip $V_{fi}^{bd}(L_{Rfi};\delta_{Li})$.

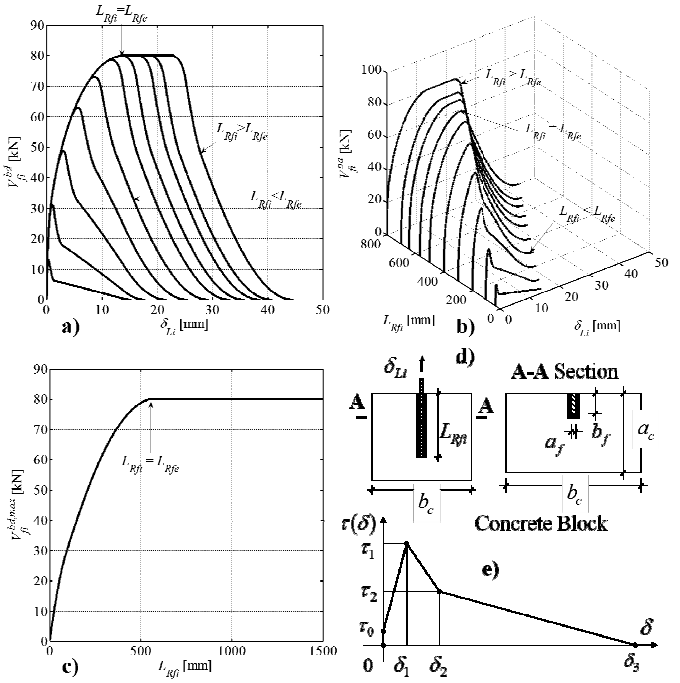

Figure 1. Bond-based behavior of a single NSM FRP strip on a concrete prism: a-b) constitutive law $V_{fi}^{bd}(L_{Rfi};\delta_{Li})$ both in a 2-D and in a 3-D representation; c) dependence of $V_{fi}^{bd,max}$ on the resisting bond length L_{Rfi}; d) concrete prism with a single NSM FRP strip and e) adopted local bond stress-slip relationship.

This latter is the curve providing the bond-based force V_{fi}^{bd} that the generic *i-th* strip, with resisting bond length L_{Rfi}, can transfer, through bond stresses, to the surrounding concrete as function of the value of the increasing imposed end slip δ_{Li} (Fig. 1a-b). The bond-based constitutive law $V_{fi}^{bd}(L_{Rfi};\delta_{Li})$ of a given NSM FRP strip depends on the following parameters (Bianco *et al.* 2009a-b) (Fig. 1d-e): strip cross section thickness a_f and width b_f; strip resisting bond length L_{Rfi}; concrete prism cross section thickness a_c and width b_c; concrete deformability E_c (which is function of the concrete compressive strength f_{cm}); strip's Young's Modulus E_f and values of bond stress (τ_0,τ_1,τ_2) and slip ($\delta_1,\delta_2,\delta_3$) defining the local bond stress-slip relationship (Fig. 1e). The analytical details necessary to evaluate the constitutive law of a given NSM FRP strip are herein omitted, for the sake of brevity, but they can be found elsewhere (Bianco *et al.* 2009a-b). The constitutive laws $V_{fi}^{bd}(L_{Rfi};\delta_{Li})$ of NSM FRP strips of different values of L_{Rfi} can be plotted both in a bi-dimensional ($V_{fi}^{bd};\delta_{Li}$) and in a three-dimensional ($V_{fi}^{bd};L_{Rfi};\delta_{Li}$) orthogonal reference system. The peak bond-transferred force $V_{fi}^{bd,max}$ increases, by increasing the value of L_{Rfi}, up to the value $V_{fi}^{bd,max}(L_{Rfe})$ corresponding to the effective resisting bond length L_{Rfe}, which is the value of L_{Rfi} beyond which any further increase of the resisting bond length L_{Rfi} does not yield any further peak load gain. In a bi-dimensional representation (Fig. 1a), the point ($V_{fi}^{bd};\delta_{Li}$) representative of the state of the NSM strip of resisting bond length L_{Rfi} moves, for increasing values of δ_{Li}, on the same branch, non-linear ascending or linear horizontal for values of $L_{Rfi} \le L_{Rfe}$ or $L_{Rfi} > L_{Rfe}$ respectively, common for each value of L_{Rfi}, as long as L_{Rfi} is larger or equal to the value of the necessary bond transfer length $L_{tr}^{bd}(\delta_{Li})$ (Bianco *et al.* 2009a-b). Where $L_{tr}^{bd}(\delta_{Li})$, function of δ_{Li} only, is the bond length that would be necessary to entirely transfer to the surrounding concrete a force equal to the one originating in the strip loaded end, due to the imposition of δ_{Li} (Bianco *et al.* 2009a). When the constitutive laws $V_{fi}^{bd}(L_{Rfi};\delta_{Li})$ of NSM FRP strips of different and increasing values of resisting bond length are represented in a three dimensional reference system, they form a continuous surface (Fig. 1b).

2.2 *Influence of each parameter on the peak bond-transferred force*

The parametric study presented in this paragraph concerns the influence of each parameter on the peak bond-transferred force for different values of L_{Rfi}. Note that each parameter was varied within a range comprehending values a little beyond those having a strict physical confirmation, in order to assess not only their influence on the physical behavior of an NSM FRP strip, but also their influence from a mere analytical-numerical standpoint (Table 1). The results of the parametric studies are reported in the following.

2.3 *Concrete and FRP Young's Modulus*

A variation of the concrete Young's Modulus E_c does not yield any variation of $V_{fi}^{bd,max}$, for whatever value of L_{Rfi} (Fig. 2a). An increase of the FRP Young's Modulus E_f yields a resisting-bond-length-dependent increase of $V_{fi}^{bd,max}$ (Fig. 2d). In fact, $V_{fi}^{bd,max}$ increases, for increasing values of E_f, with a rate that is as larger as larger is the value of L_{Rfi}. Moreover, the curves providing $V_{fi}^{bd,max}$ as function of E_f and L_{Rfi} show two phases: a first one, coincident for all of the values of L_{Rfi}, characterized by a larger value of the increment $dV_{fi}^{bd,max}/dE_f$ of $V_{fi}^{bd,max}$ for an increment of E_f and a second phase, different for each value of L_{Rfi}, characterized by a smaller value of the increasing rate $dV_{fi}^{bd,max}/dE_f$. Along the first of those phases, the larger value of $dV_{fi}^{bd,max}/dE_f$ is due to the fact that, for each value of L_{Rfi}, and for each value of E_f, the resisting bond length is larger or equal to the corresponding value of the effective resisting bond length $L_{Rfe}(E_f)$, which is independent of the value of L_{Rfi}, and so the largest value of force that an NSM FRP strip characterized by that value of E_f could transfer by bond can actually be attained (see also Fig. 1c). Along the second phase, since L_{Rfi} is smaller than the corresponding value of the effective resisting bond length $L_{Rfe}(E_f)$, the largest value of bond transferred force cannot be attained.

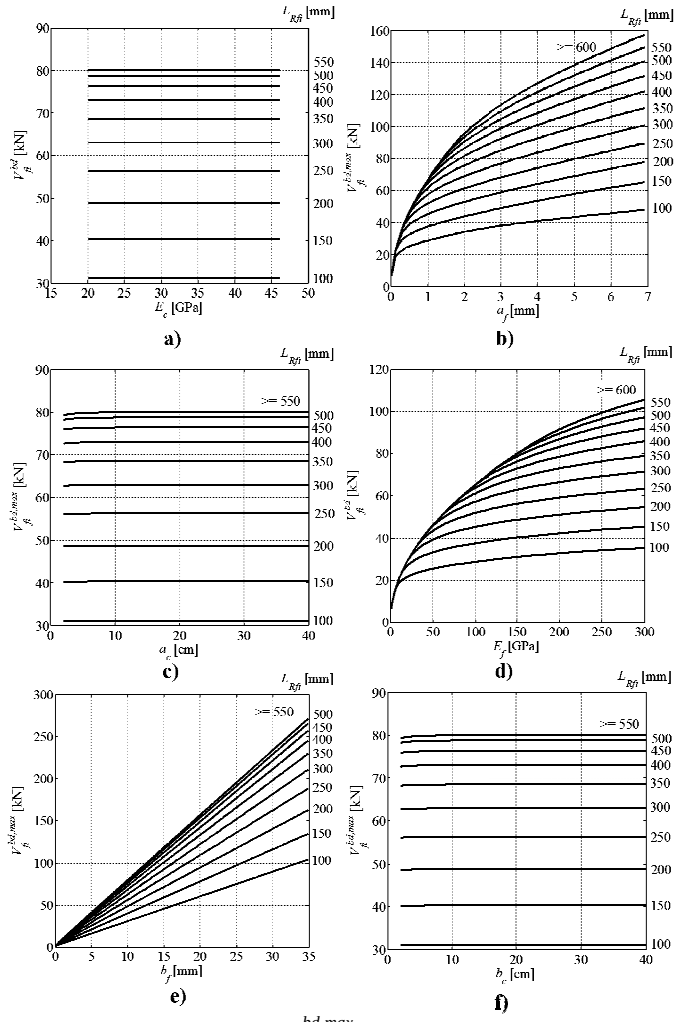

Figure 2. Variation of $V_{fi}^{bd,max}$ as function of: a) concrete Young's Modulus E_c, b) strip thickness a_f, c) concrete prism thickness a_c, d) FRP Young's Modulus E_f, e) strip width b_f and f) concrete prism width b_c.

2.4 *Geometrical dimensions of both FRP strip and concrete prism*

An increase of the strip cross section dimensions (Fig. 2b,e), either a_f or b_f, yields a resisting-bond-length-dependent increase of $V_{fi}^{bd,max}$. In particular, for the case of the strip cross section thickness a_f, the curves providing $V_{fi}^{bd,max}$ as function of a_f, for different values of L_{Rfi}, are superimposed as long as it is $L_{Rfi} \geq L_{Rfe}(a_f)$ and present a different increasing rate, the larger as larger L_{Rfi} is, for values of $L_{Rfi} < L_{Rfe}(a_f)$. A variation of the prism cross section dimensions, either a_c or b_c, does not yield any appreciable variation of $V_{fi}^{bd,max}$, for whatever value of L_{Rfi} (Fig. 2c,f).

2.5 *Parameters defining the local bond stress-slip relationship*

The peak bond-transferred load $V_{fi}^{bd,max}$ increases by increasing the resisting bond length up to a certain value beyond which any further increase does not produce any further gain in terms of resistance (Fig. 1c). That threshold value of length, according to the terminology already adopted for the Externally Bonded Reinforcement (EBR), is herein labeled as effective resisting bond length L_{Rfe}. Note that for the values of the mechanical parameters herein adopted for the reference strip (Table 1), it is L_{Rfe} = 486 *mm*.

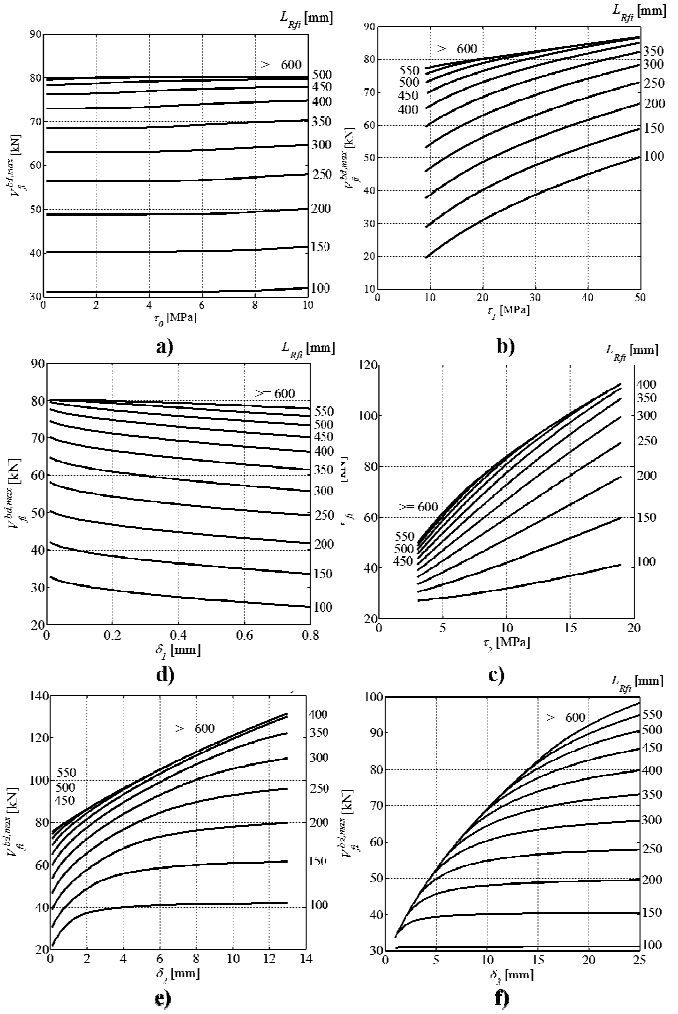

Figure 3. Influence of the parameters defining the local bond stress-slip relationship on the peak force $V_{fi}^{bd,max}$ that a single NSM FRP strip can transfer, through bond stresses, to the surrounding concrete.

As regards the influence of the parameters characterizing the local bond stress-slip relationship, it arises that $V_{fi}^{bd,max}$ is marginally affected when a realistic range of τ_0 values is considered, for whatever value of L_{Rfi} (Fig. 3a). The peak bond-transferred force $V_{fi}^{bd,max}$ increases with a resisting-bond-length-dependent-rate by increasing the value of either τ_1 or τ_2. In particular, $V_{fi}^{bd,max}$ increases by increasing τ_1 with a rate that is larger as shorter is the value of L_{Rfi} while $V_{fi}^{bd,max}$ increases by increasing τ_2 with a rate that is larger as larger is the value of L_{Rfi} (Fig. 3b-c). $V_{fi}^{bd,max}$ decreases for increasing values of δ_1 with a resisting-bond-length-dependent-rate: in fact, the larger the value of L_{Rfi}, the smaller is the rate with which $V_{fi}^{bd,max}$ decreases for increasing values of δ_1 (Fig. 3d). An increase of either δ_2 or δ_3 (Fig. 3e-f) yields an increase of $V_{fi}^{bd,max}$ with a rate that is resisting-bond-length dependent. In particular, for the case of δ_3, the curves providing $V_{fi}^{bd,max}$ as function of δ_3, for the different values of L_{Rfi}, are superimposed, presenting the same trend, as long as L_{Rfi} is larger or equal to $L_{Rfe}(\delta_3)$. Note that, for all of the parameters analyzed, the curves providing $V_{fi}^{bd,max}$ as

function of the generic parameter for the various values of L_{Rfi} tend, by increasing the value of L_{Rfi}, to a limit curve. Moreover, for values of L_{Rfi} larger than a certain value, the curves providing $V_{fi}^{bd,max}$ as function of the generic parameter are all superimposed to the envelope one.

3 COMPREHENSIVE BEHAVIOR OF A SINGLE NSM FRP STRIP

3.1 *Comprehensive constitutive law*

The model was also applied to study the comprehensive behavior of a single NSM FRP strip, mounted on a concrete prism and subjected to an increasing imposed end slip. For this purpose, the possibilities of both concrete semi-conical tensile fracture and strip tensile rupture were also taken into account. Typically, according to the model herein adopted (Bianco 2008, Bianco et al. 2009a), increasing the imposed end slip to the single NSM FRP strip, co-axial and progressively larger semi-conical concrete fractures form in sequence around the strip since the very first load steps (Fig. 4b,c). At the same time, at the occurrence of each concrete semi-conical fracture, the initial value of the resisting bond length L_{Rfi}^{0} progressively reduces. Moreover, due to the formation of successive co-axial semi-conical fracture surfaces around the strip, the resulting concrete fracture envelope surface, which corresponds to the last and larger semi-conical surface, starting from the loaded end, progressively penetrates within the concrete prism (Fig. 4c). It can happen that the vertex of the last semi-conical concrete fracture surface places midway between the loaded and free end or reaches this latter. Moreover, contextually at the occurrence of each of those concrete fractures, the point representative of the state of the strip, with coordinates $(V_{fi};L_{Rfi};\delta_{Li})$ leaps, for a constant value of δ_{Li}, from the bond-based constitutive law $V_{fi}^{bd}(L_{Rfi}^{n};\delta_{Li})$ of the previous value of resisting bond length L_{Rfi}^{n} to the one corresponding to the new value of resisting bond length L_{Rfi}^{n+1} (Fig. 5). The leap of the point $(V_{fi};L_{Rfi};\delta_{Li})$ representative of the state of the strip from one bond-based constitutive law to the other is only visible in a three dimensional representation, as long as the concrete fracture is superficial (Fig. 5b,e). Where superficial concrete fracture means that, each time the point representative of the state of the strip leaps from one bond-based constitutive law to another, the updated value of L_{Rfi} is larger or equal to the necessary bond transfer length $L_{tr}^{bd}(\delta_{Li})$ (Fig. 5b,e). On the contrary, the leap of the point $(V_{fi};L_{Rfi};\delta_{Li})$ representative of the state of the strip from one bond-based constitutive law to the other is also visible in a two dimensional representation, as long as the concrete fracture is deep (Fig. 5a,d). Where deep concrete fracture means that, when the point representative of the state of the strip leaps to the last bond-based constitutive law, the new value of L_{Rfi} is smaller than the necessary bond transfer length $L_{tr}^{bd}(\delta_{Li})$ corresponding to the current value of δ_{Li} (Fig. 5a,d).

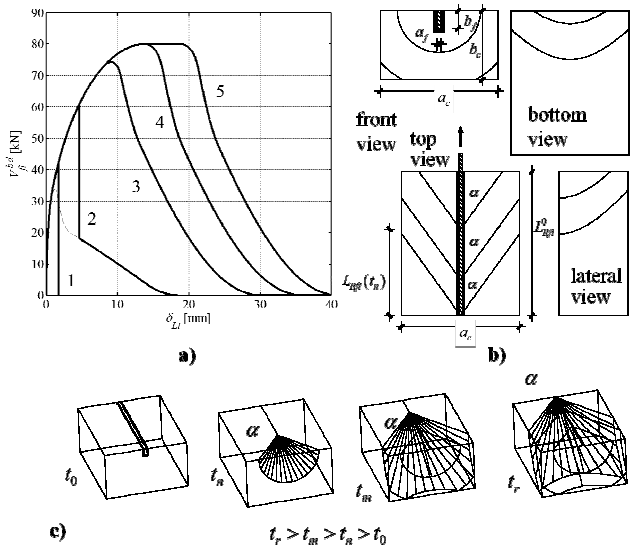

Figure 4. Comprehensive behavior of a single NSM FRP strip: a) possible comprehensive constitutive law types, b) successive and co-axial semi-conical fracture surfaces occurring around the NSM strip and c) progressive reduction of the resisting bond length and penetration of the semi-conical fracture within the concrete prism.

When the point $(V_{fi};L_{Rfi};\delta_{Li})$ representative of the state of the strip eventually leaps on the bond-based constitutive law of a strip with null resisting bond length, the ultimate configuration is characterized by a semi-conical concrete fracture whose vertex coincides with the strip free end. It can also happen that, after an initial semi-conical concrete fracture, at a certain point of the loading process, the strip ruptures and the point $(V_{fi};L_{Rfi};\delta_{Li})$ representative of the state of the strip abruptly falls on the plane $(L_{Rfi};\delta_{Li})$ and the relevant force V_{fi} vanishes (Fig. 5c,f). Note that, whatever the failure mode characterizing the specific single NSM FRP strip, due to the continuity characterizing the surface envelope of the bond-based constitutive laws (Fig. 1b), it always exists an equivalent value of the resisting bond length L_{Rfi}^{eq}, which is the value of the resisting bond length to which corresponds a bond-based constitutive law $V_{fi}^{bd}(L_{Rfi}^{eq};\delta_{Li})$ whose peak value $V_{fi}^{bd,max}$ is equal to the peak value V_{fi}^{max} of the comprehensive constitutive law $V_{fi}(L_{Rfi}^{0};\delta_{Li})$ of the initial value of the resisting bond length L_{Rfi}^{0} (Fig. 5). Ultimately, the comprehensive constitutive law of a single NSM FRP strip mounted on a concrete prism can be one of the following types (Fig. 4a): (1) either rupture of the strip, preceded or not by a superficial semi-conical fracture, or deep concrete semi-conical fracture up to the free end; (2) deep concrete semi-conical fracture with the concrete fracture stopping midway between loaded and free end; superficial concrete fracture with the last value assumed by L_{Rfi} shorter (3), equal (4) or larger (5) than the effective resisting bond length.

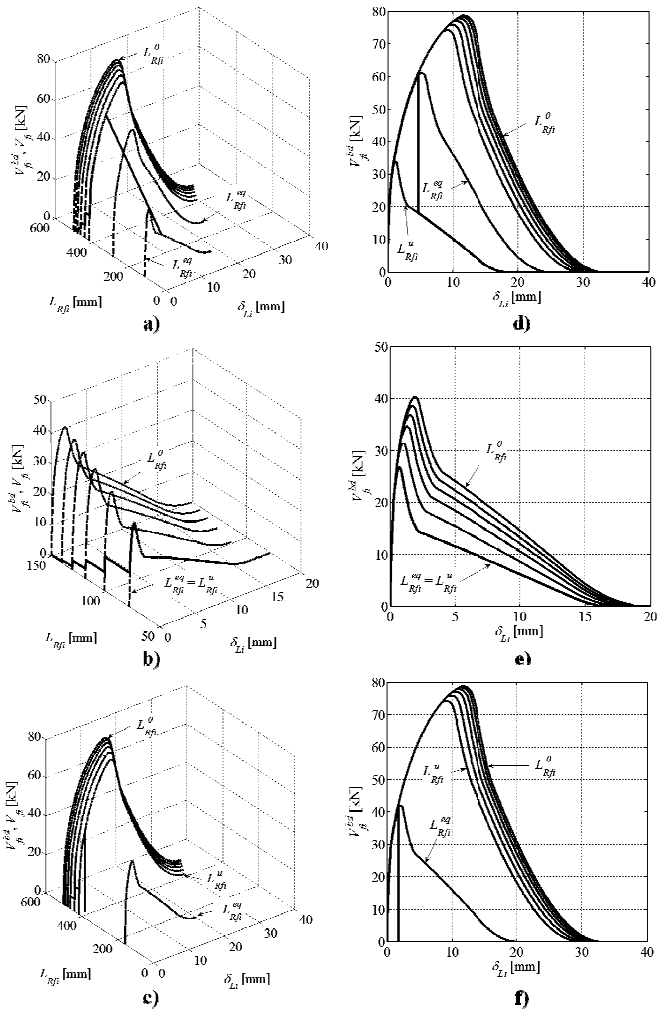

Figure 5. Comprehensive constitutive law $V_{fi}(L_{Rfi};\delta_{Li})$ of a single NSM FRP strip: a,d) deep concrete fracture, b,e) superficial concrete fracture and c,f) strip rupture after a superficial concrete fracture.

3.2 *Influence of each parameter on the peak value of the comprehensive constitutive law*

In this section, a parametric study, regarding the influence of each of the geometrical-mechanical parameters on the peak value V_{fi}^{max} of the comprehensive constitutive law $V_{fi}(L_{Rfi};\delta_{Li})$ of a single NSM FRP strip, is presented. Note that even in this case, each parameter was varied within a range comprehending values a little beyond those having a strict physical confirmation, in order to asses not only their influence on the physical behavior of an NSM FRP strip, but also their influence from a mere analytical-numerical standpoint. Besides the parameters already introduced in the previous paragraph, the comprehensive behavior of a single NSM FRP strip also depends on (Table 1): strip tensile strength f_{fu}, angle between axis and generatrices of the concrete semi-conical fracture surface α (Fig. 4b,c). Among the derived parameters, the concrete average tensile strength f_{ctm}, function of f_{cm} is obtained, in the present work, as function of the concrete compressive strength by means of the formulae reported by the CEB Fip Model Code 90.

3.2.1 *FRP strip mechanical properties*

The curves representing the variation of V_{fi}^{max} with respect to the FRP strip tensile strength f_{fu} present a bi-linear elastic-perfectly-plastic behavior for whatever value of L_{Rfi} (Fig. 6a). Along the first linear branch, the failure mode is rupture of the strip, due to the reduced value of the strip tensile strength $V_{fi}^{tr}(a_f \cdot b_f \cdot f_{fu})$. Along the second linear branch, the failure mode is governed by superficial concrete fracture for the shorter values of the initial resisting bond length and by deep concrete fracture for the larger values of the initial resisting bond length. Note that, since the value of f_{fu} does not affect the pure bond-based behavior of a NSM FRP strip, for a given value of L_{Rfi}^{0} and for values of f_{fu} larger than the one by which the strip no longer ruptures, the ultimate configuration and the relevant peak load V_{fi}^{max} no longer change by increasing f_{fu}. Note also that the curves providing the values of V_{fi}^{max} as function of f_{fu} for the various values of L_{Rfi}^{0} tend to a limit curve that defines the envelope of the various curves. In fact, for the values herein assumed for the other parameters (Table 1), the curve providing V_{fi}^{max} as function of f_{fu} is exactly the same regardless of the value assumed by L_{Rfi}^{0} for values of L_{Rfi}^{0} larger than 400 mm (Fig. 6a). The curves $V_{fi}^{max}(E_f;L_{Rfi}^{0})$ providing V_{fi}^{max} as function of the strip Young's Modulus E_f show a pseudo bi-linear trend for any value of L_{Rfi}^{0} (Fig. 6d). Along the first branch, the ultimate behavior is characterized by superficial concrete fracture and, since the equivalent values of the resisting bond length are larger or equal to the corresponding values of the effective resisting bond length $L_{Rfi}^{eq}(E_f) \geq L_{Rfe}(E_f)$, the same trend characterizing the pure-bond behavior can be found (compare Fig. 6d and Fig. 2d). Nevertheless, due to the reduction of L_{Rfi}^{0} ascribed to the superficial concrete fracture, the maximum value of V_{fi}^{max}, for a given value of L_{Rfi}^{0}, is smaller than the maximum of $V_{fi}^{bd,max}$ for the same value of L_{Rfi}^{0}. The pseudo horizontal branches of the curves $V_{fi}^{max}(E_f;L_{Rfi}^{0})$ correspond, for the shorter values of L_{Rfi}^{0} ($< 350\ mm$), to a deep concrete fracture failure mode and, for the longer values of L_{Rfi}^{0} ($\geq 350\ mm$), to the rupture of the strips. The horizontal branches of the curves $V_{fi}^{max}(E_f;L_{Rfi}^{0})$ tend, for increasing values of L_{Rfi}^{0}, to the limit curve corresponding to the value of the strip rupture capacity ($V_f^{tr} = 42.0\ kN$ for the values herein assumed for the other parameters). Note that, on the horizontal branches of the curves $V_{fi}^{max}(E_f;L_{Rfi}^{0})$ for the shorter values of L_{Rfi}^{0}, despite a fluctuation, due to concrete fracture, around an average value, V_{fi}^{max} is almost constant even if, by increasing E_f, concrete fracture deepens and L_{Rfi}^{eq} progressively becomes a smaller portion of L_{Rfi}^{0}. This is due to the fact that, by increasing E_f, the values of the resisting bond lengths necessary to transfer the same value of $V_{fi}^{bd,max}$ increase (Bianco 2008).

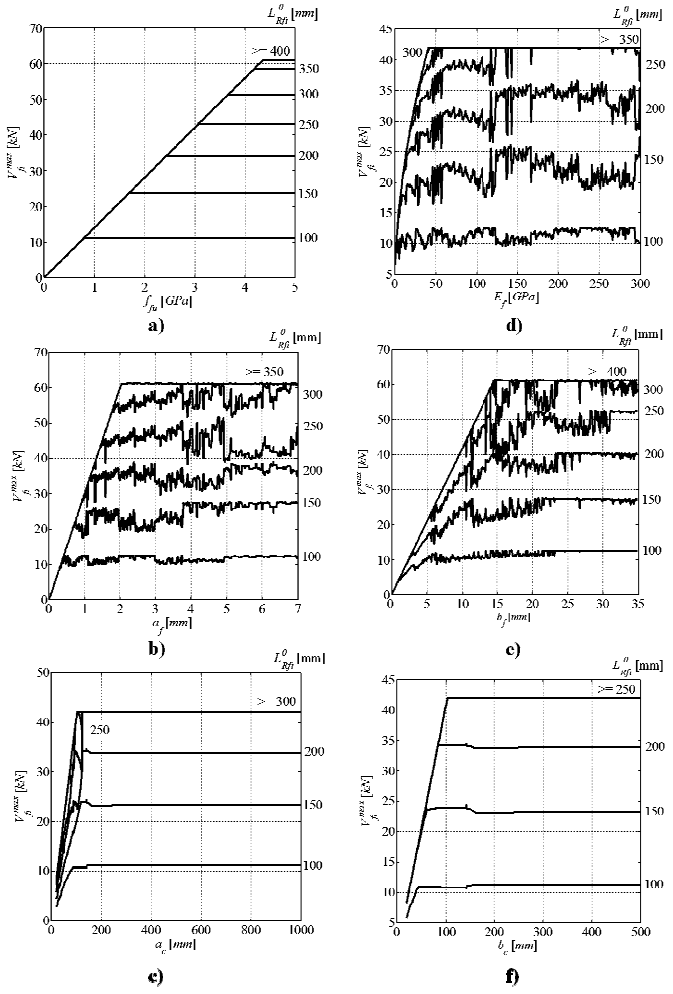

Figure 6. Variation of $V_{fi}^{max}(L_{Rfi}^{0})$, as function of: FRP's a) tensile strength f_{fu} and d) Young's Modulus E_f, strip cross section b) thickness E_f and e) width E_f and concrete prism cross section c) thickness a_c and f) width b_c.

3.2.2 *FRP strip cross-section dimensions*

The curves $V_{fi}^{max}(a_f;L_{Rfi}^{0})$ and $V_{fi}^{max}(b_f;L_{Rfi}^{0})$ providing the value of V_{fi}^{max} as function of the strip cross-section dimensions show, for whatever value of L_{Rfi}^{0}, a pseudo bi-linear trend (Fig. 6b,e). Along the first branch of those curves, due to the reduced area of the strip cross-section, the failure mode is rupture of the strip and V_{fi}^{max} increases linearly for increasing values of either a_f or b_f. Along the second branch of those curves, the ultimate configuration is of the mixed-semi-cone-plus-debonding type and, for the shorter values of L_{Rfi}^{0}, the failure mode is superficial concrete fracture while for the longer values of L_{Rfi}^{0}, the failure mode is deep concrete fracture. The horizontal branches of those curves tend, for increasing values of L_{Rfi}^{0}, to the limit curve corresponding to the value of approximately V_{fi}^{max} = 62.0 *kN*. From a certain value of L_{Rfi}^{0} on ($L_{Rfi}^{0} \geq 350$ *mm* for a_f and $L_{Rfi}^{0} \geq 400$ *mm* for b_f), the curves above overlap on the limit curve and the maximum value of V_{fi}^{max} does not further increase for increasing values of L_{Rfi}^{0} since the maximum value of force that the concrete prism, with given geometrical/mechanical properties, can stand, has been attained.

3.2.3 *Concrete prism cross-section dimensions*

The curves $V_{fi}^{max}(a_c;L_{Rfi}^{0})$ and $V_{fi}^{max}(b_c;L_{Rfi}^{0})$ providing the value of V_{fi}^{max} as function of the concrete prism cross section dimensions (Fig. 4b) show, for any value of L_{Rfi}^{0}, a pseudo bi-linear trend (Fig. 6c,f). Along the first branch of those curves, since the prism cross-section is small, the successive coaxial semi-conical fracture surfaces, whose axis is a progressively larger amount of L_{Rfi}^{0}, soon intersect the concrete prism faces (Fig. 4b,c). Thus, the concrete semi-conical fracture capacity V_{fi}^{cf}, obtained integrating the concrete average tensile strength throughout the surface resulting from the intersection of the right semi-conical surface with the prism faces, is very low (Bianco *et al.* 2009a-b). Due to the small value of the concrete fracture capacity, along the first branch of the curves $V_{fi}^{max}(a_c;L_{Rfi}^{0})$ and $V_{fi}^{max}(b_c;L_{Rfi}^{0})$, the failure mode is very deep concrete fracture with the vertex of the last semi-conical fracture surface reaching the strip free end (Fig. 4b,c). Along the second branch of those curves, for increasing values of either a_c or b_c, and for the shorter values of L_{Rfi}^{0}, concrete fracture becomes, as long as the largest semi-conical surface intersects the prism walls, progressively more superficial. From the value of either a_c or b_c, in correspondence of which the largest semi-conical surface no longer intersects the prism faces, the ultimate configuration and the corresponding value of V_{fi}^{max}, for a given value of L_{Rfi}^{0}, remains practically unchanged. Along the second branch of those curves, for values of L_{Rfi}^{0} larger than a certain value ($L_{Rfi}^{0} \geq 300$ *mm* for a_c and $L_{Rfi}^{0} \geq 250$ *mm* for b_c), the failure mode is governed by the strip rupture and those branches overlap on the limit curve corresponding to the value of $V_{fi}^{max} = V_f^{tr}$ = 42.0 *kN* (Fig. 6c,f).

3.2.4 *Concrete mechanical properties*

The curves $V_{fi}^{max}(\alpha;L_{Rfi}^{0})$ and $V_{fi}^{max}(f_{cm};L_{Rfi}^{0})$ providing the value of V_{fi}^{max} as function of either of the parameters defining the concrete mechanical properties, either f_{cm} or α, show, for any value of L_{Rfi}^{0}, a nonlinear trend in which, in the most general case, three successive branches can be singled out (Fig. 7a,b). Along the first branch, for small values of either f_{cm} or α, since concrete mechanical properties are very low, concrete fracture is so deep to reach the strip free extremity. This first branch of the curve is continuous since, going from one value to the other of the parameter analyzed (f_{cm} or α), the peak value V_{fi}^{max} is always equal to the concrete semi-conical fracture capacity V_{fi}^{cf} associated to the maximum semi-conical surface that can form inside the concrete prism (Fig. 4bc). Along this first branch, the concrete fracture capacity $V_{fi}^{cf}(L_{Rfi}^{0})$, integral of f_{ctm} on the maximum semi-conical surface, varies with continuity for an increase of either $f_{ctm}(f_{cm})$ or α. In this latter case, $V_{fi}^{cf}(L_{Rfi}^{0})$ varies with continuity if either the maximum semi-conical sur-

face intersects (for larger values of α) or not (for smaller values of α) the concrete prism faces (Fig. 4). By increasing the values of either f_{cm} or α, concrete fracture progressively becomes more superficial and the equivalent value of the resisting bond length becomes a progressively larger portion of L_{Rfi}^{0}. Along the second branch of the curves $V_{fi}^{max}(\alpha;L_{Rfi}^{0})$ and $V_{fi}^{max}(f_{cm};L_{Rfi}^{0})$ the ultimate configuration is of the mixed-semi-cone-plus-debonding type. Such second branch is characterized by a two-fold fluctuation of the values V_{fi}^{max}, by varying either one of the parameters analyzed (f_{cm} or α), and for a given value of L_{Rfi}^{0}, around the values corresponding to an average and continuous curve: a micro-fluctuation ad a macro-fluctuation. The former is a fluctuation that has a numerical origin and is due to the way the concrete semi-conical fracture phenomenon was modeled (Bianco 2008 and Bianco *et al.* 2009a). The latter, which consists in the presence of some steps upwards, is due to the fact that, for increasing values of the concrete mechanical properties, the number of successive reductions of L_{Rfi}^{0} (Fig. 4), contextual to the occurrence of successive concrete semi-conical fractures, reduces for increasing values of either of the parameters analyzed (f_{cm} or α). Along the third branch, attained indeed only for the larger values of L_{Rfi}^{0} and for increasing values of the concrete mechanical properties, the ultimate configuration is composed of a superficial semi-conical concrete fracture followed by the rupture of the strip itself. Such third branch is therefore horizontal and equal to the value of the strip rupture capacity that, for the values herein assumed for the other parameters, is equal to 42.0 *kN*. The curves $V_{fi}^{max}(\alpha;L_{Rfi}^{0})$ and $V_{fi}^{max}(f_{cm};L_{Rfi}^{0})$, for increasing values of L_{Rfi}^{0}, progressively become closer to each other up to overlapping on a limit curve for values of L_{Rfi}^{0} larger than a certain limit value that, for the values herein assumed for the other parameters, is equal to 450 *mm* for α and to 300 *mm* for f_{cm}. Note that the curves $V_{fi}^{max}(f_{cm};L_{Rfi}^{0})$ start from a value of f_{cm} equal to $8.0\,MPa$. This is due to the fact that the concrete average tensile strength f_{ctm} was calculated from the concrete average compressive strength by means of the formulae reported by the CEB-FIP Model Code 90 that provide values of f_{ctm} larger than zero for values of f_{cm} larger than $8.0\,MPa$. Note also that, if either f_{cm} or α were increased infinitely, for a given value of L_{Rfi}^{0}, the value of V_{fi}^{max} would tend to the corresponding bond-based peak load $V_{fi}^{bd,max}(L_{Rfi}^{0})$, as long as this latter is smaller than the strip rupture capacity.

3.2.5 *FRP strip initial resisting bond length*

The curve $V_{fi}^{max}(L_{Rfi}^{0})$ providing the value of V_{fi}^{max} as function of the value of L_{Rfi}^{0} also presents a pseudo bi-linear trend (Fig. 7c). Along the first branch, the failure mode is concrete semi-conical fracture, either superficial or deep, with an ultimate configuration of the mixed-semi-cone-plus-debonding type. Along the second branch, the failure mode is rupture of the strip. Note that even in this case, as for the pure bond behavior (see previous paragraph), it is possible to single out an effective value of L_{Rfi}^{0}, which can be labeled as comprehensive effective resisting bond length L_{Rfe}^{0}, beyond which any further increase of L_{Rfi}^{0} does not produce any further gain in terms of V_{fi}^{max}. In general, the comprehensive effective resisting bond length L_{Rfe}^{0}, due to the occurrence of one of either concrete fracture or strip rupture, is shorter than the effective resisting bond length L_{Rfe} (see also Fig. 1c).

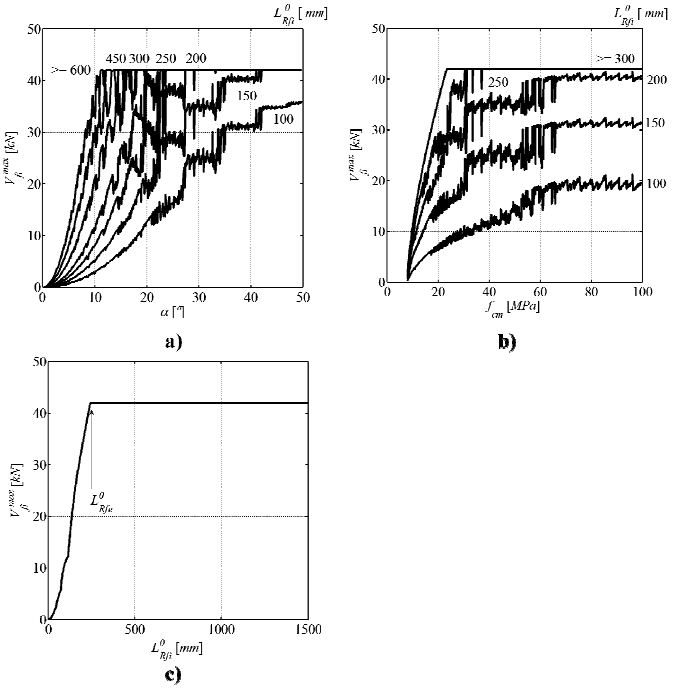

Figure 7. Variation of $V_{fi}^{max}(L_{Rfi}^{0})$, as function of: a) the angle between axis and generatrices of the semi-conical concrete fracture surface α, b) concrete average compressive strength f_{cm} and c) initial resisting bond length L_{Rfi}^{0}.

3.2.6 *Parameters defining the local bond stress-slip relationship*

The peak force V_{fi}^{max} that an NSM FRP strip of a given resisting bond length L_{Rfi}^{0} can resist does not vary by increasing the value of the parameter τ_0, characterizing the adopted local bond stress-slip relationship, for whatever value of the initial resisting bond length L_{Rfi}^{0} (Fig. 8a). Actually, the parameter τ_0 was already found not to affect the peak bond-transferred force $V_{fi}^{bd,max}$ (Fig. 3a). Nonetheless, due to the occurrence of other phenomena such as either concrete tensile fracture or strip rupture, the peak value of the curve $V_{fi}^{max}(\tau_0;L_{Rfi}^{0})$ is lower than the peak value of the corresponding curve $V_{fi}^{bd,max}(\tau_0;L_{Rfi}^{0})$ for a value of $L_{Rfi} = L_{Rfi}^{0}$. For the shorter values of L_{Rfi}^{0}, the failure mode is governed by concrete tensile fracture, either superficial or deep, while, for values of L_{Rfi}^{0} larger or equal to a certain value, the failure mode is the strip rupture. The values of the parameters τ_1 and τ_2 have a negli-

gible influence on the peak value of the comprehensive constitutive law of a NSM FRP strip of a given resisting bond length L_{Rfi}^{0} (Fig. 8b,c). In fact, the curves $V_{fi}^{max}(\tau_1;L_{Rfi}^{0})$ and $V_{fi}^{max}(\tau_2;L_{Rfi}^{0})$ do not show appreciable variations, by increasing either τ_1 or τ_2, for any value of L_{Rfi}^{0}. For the shorter values of L_{Rfi}^{0}, the failure mode is governed by concrete tensile fracture, either superficial or deep while, for values of L_{Rfi}^{0} larger or equal to a certain value, the failure mode is the strip rupture. Each of the bond slip values characterizing the local bond stress-slip relationship, either δ_1 or δ_2 or δ_3, has a marginal influence on the peak value of the comprehensive constitutive law of a NSM FRP strip of a given value of the initial resisting bond length L_{Rfi}^{0} (Fig. 8d-f). For the shorter values of L_{Rfi}^{0}, the failure mode is governed by concrete tensile fracture, either superficial or deep while, for values of L_{Rfi}^{0} larger or equal to a certain value, the failure mode is the strip rupture. Note that the curves providing V_{fi}^{max} as function of either of the various parameters defining the local bond stress-slip relationship tend, for increasing values of L_{Rfi}^{0}, to overlap to the limit curve corresponding to the strip rupture $V_{fi}^{max} = V_f^{tr}$.

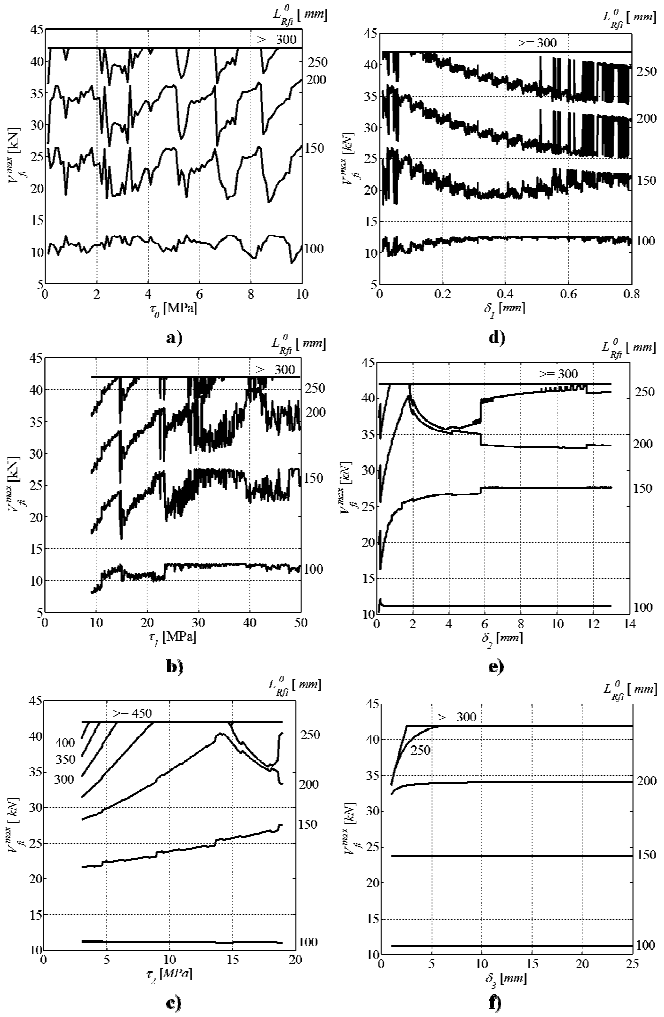

Figure 8. Variation of the peak force that a single strip can comprehensively transfer to the surrounding concrete $V_{fi}^{max}(L_{Rfi}^{0})$, as function of the parameters defining the adopted local bond stress-slip relationship.

Table 1. Input parameters values for the parametric studies .

	RS	RoV		RS	RoV
E_f [GPa]	150.0	0-300	L_{Rfi} [cm]	4.0	0-150
f_{fu} [GPa]	3.0	0-5.0	τ_0 [MPa]	2.0	0.5-10
f_{cm} [MPa]	35.0	20-70	τ_1 [MPa]	20.1	9.0-50
α [°]	28.5	0-50	τ_2 [MPa]	9.0	3.0-19
a_f [mm]	1.4	0-7.0	δ_1 [mm]	0.07	0.05-0.8
b_f [mm]	10.0	0-35	δ_2 [mm]	0.83	0.2-13
a_c [cm]	15.0	2-40	δ_3 [mm]	14.1	2.0-25
b_c [cm]	15.0	2-40			

RS = Reference Strip; RoV = Range of Variation

4 CONCLUSIONS

A recently developed mechanical model was herein applied to carry out parametric studies on the influence of each parameter on the force transferred by a single NSM FRP strip to a prism of plain concrete. The dependence of most of the input geometrical-mechanical parameters on the peak force that a single NSM FRP strip can transfer is strongly nonlinear. A variation of each of the parameters defining the local bond stress-slip relationship yields a negligible variation of the peak force transferred by a single NSM FRP strip. In fact, the premature occurrence of either concrete semi-conical fracture or strip rupture does not allow to attain the peak bond-transferred force that a single strip, with the given value of initial resisting bond length, would be capable to attain.

5 REFERENCES

Bianco, V., (2008). "Shear Strengthening of RC beams by means of NSM FRP strips: experimental evidence and analytical modeling", PhD Thesis, Dept. of Structural Engrg. and Geotechnics, Sapienza University of Rome, Italy, submitted on December 2008.

Bianco, V., Barros, J.A.O., Monti, G., (2009a). "Three dimensional mechanical model for simulating the NSM FRP strips shear strength contribution to RC beams", Engineering Structures, 31(4), April 2009, 815-826.

Bianco, V., Barros, J.A.O., Monti, G., (2009b). "Bond Model of NSM FRP strips in the context of the Shear Strengthening of RC beams", ASCE Journal of Structural Engineering, 135(6), June 2009.

CEB-FIP Model Code 90, (1993) Bulletin d'Information N° 213/214, Final version printed by Th. Telford, London, (1993; ISBN 0-7277-1696-4; 460 pages).